J|A|C|S ARTICLES

Published on Web 07/19/2010

Investigation of Methanol Oxidation over Au/Catalysts Using Operando IR Spectroscopy: Determination of the Active Sites, Intermediate/Spectator Species, and Reaction Mechanism

Séverine Rousseau,[†,§] Olivier Marie,*[,†] Philippe Bazin,[†] Marco Daturi,[†] Stéphane Verdier,[‡] and Virginie Harlé[‡]

Laboratoire Catalyse et Spectrochimie, ENSICAEN, Université de Caen, CNRS, 6 Bd Maréchal Juin, 14050 Caen, France, and Rhodia Recherches, 52 Rue de la Haie Coq, 93308 Aubervilliers Cedex, France

Received April 6, 2010; E-mail: marieo@ensicaen.fr

Abstract: FTIR spectroscopy coupled with mass spectrometry has been used to study the mechanism of methanol oxidation at low temperatures on nanostructured Au/CeO_2 and Au/TiO_2 catalysts. Activity and selectivity toward CO_2 have been investigated through simultaneous analysis of adsorbed surface species and gaseous species, and some key steps in the oxidation pathway, active sites, and intermediate species are proposed. Among the detected species, some kinds of methoxy species formed on the support were identified as intermediates, which further transform into formates whose oxidation was found to be the rate-determining step for the reaction. The role of the support and the noble metal in the mechanism are revealed using operando spectroscopy.

1. Introduction

In the frame of air depollution, several targets (such as automobile cockpits, working or public frequented indoor halls, restricted areas, refrigerated cells, domestic environment, etc.) require more efficient compounds than activated carbon absorbers. The aim being not only to remove the atmospheric pollutants but also to transform them into inert species, an inexpensive catalytic process efficient at room temperature (and even below) under atmospheric conditions was investigated as a challenge. Here, the complete oxidation of methanol (CH_3OH) chosen as model volatile organic compound (VOC) and its mechanism in heterogeneous catalysis are reported. The oxidizing agent being the dioxygen naturally present in the ambient air, the total methanol oxidation stoichiometry is described by the following equation:

$$CH_3OH + \frac{3}{2}O_2 \rightarrow CO_2 + 2H_2O \qquad (1)$$

Regarding the nature of potential candidates for active catalysts, a brief survey of the literature data relative to air pollution abatement indicates that the presence of CeO_2,[1−12] TiO_2,[2,7,12,13] or even $Ce_xTi_{(1-x)}O_2$[14,15] as metal oxide supports greatly enhances the efficiency of "classical" Al_2O_3 supported noble metal catalysts for VOC total oxidation. Not only do supported noble metals such as Pd, Pt, Ag[12,16−20] provide active sites for oxidation reaction, but also transition metals (such as Cu) supported onto the previously selected oxides[3,21−23] are reported to be efficient, especially for the CO preferential oxidation. Indeed, the CO preferential oxidation reaction (known as the PROX reaction) has been the subject of many efforts in both the academic and the industrial world due to the high

† Université de Caen.
‡ Rhodia Recherches.
§ Current address: PSA Peugeot Citroën - Centre Technique de Vélizy, Route de Gisy, 78943 Vélizy Villacoublay, France.

(1) Gluhoi, A. C.; Lin, S. D.; Nieuwenhuys, B. E. *Catal. Today* **2004**, *90*, 175–181.
(2) Liu, S. Y.; Yang, S. M. *Appl. Catal., A* **2008**, *334*, 92–99.
(3) Liu, W. *China Particuol.* **2005**, *3*, 383–394.
(4) Scirè, S.; Minicò, S.; Crisafulli, C.; Satriano, C.; Pistone, A. *Appl. Catal., B* **2003**, *40*, 43–49.
(5) Shen, Y.; Yang, X.; Wang, Y.; Zhang, Y.; Zhu, H.; Gao, L.; Jia, M. *Appl. Catal., B* **2008**, *79*, 142–148.
(6) Sheng, P. Y.; Bowmaker, G. A.; Idriss, H. *Appl. Catal., A* **2004**, *261*, 171–181.
(7) Solsona, B. E.; Garcia, T.; Jones, C.; Taylor, S. H.; Carley, A. F.; Hutchings, G. J. *Appl. Catal., A* **2006**, *312*, 67–76.
(8) Andreeva, D.; Petrova, P.; Ilieva, L.; Sobczak, J. W.; Abrashev, M. V. *Appl. Catal., B* **2008**, *77*, 364–372.
(9) Centeno, M. A.; Paulis, M.; Montes, M.; Odriozola, J. A. *Appl. Catal., A* **2002**, *234*, 65–78.
(10) Liotta, L. F.; Di Carlo, G.; Longo, A.; Pantaleo, G.; Venezia, A. M. *Catal. Today* **2008**, *139*, 174–179.
(11) Milone, C.; Fazio, M.; Pistone, A.; Galvagno, S. *Appl. Catal., B* **2006**, *68*, 28–37.
(12) Rojluechai, S.; Chavadej, S.; Schwank, J. W.; Meeyoo, V. *Catal. Commun.* **2007**, *8*, 57–64.
(13) Damyanova, S.; Cubeiro, M. L.; Fierro, J. L. G. *J. Mol. Catal. A: Chem.* **1999**, *142*, 85–100.
(14) Gennequin, C.; Lamallem, M.; Cousin, R.; Siffert, S.; Aïssi, F.; Aboukaïs, A. *Catal. Today* **2007**, *122*, 301–306.
(15) Lamallem, M.; Ayadi, H. E.; Gennequin, C.; Cousin, R.; Siffert, S.; Aïssi, F.; Aboukaïs, A. *Catal. Today* **2008**, *137*, 367–372.
(16) Choudhary, V. R.; Samanta, C.; Choudhary, T. V. *Appl. Catal., A* **2006**, *308*, 128–133.
(17) Menegazzo, F.; Burti, P.; Signoretto, M.; Manzoli, M.; Vankova, S.; Boccuzzi, F.; Pinna, F.; Strukul, G. *J. Catal.* **2008**, *257*, 369–381.
(18) Monyanon, S.; Pongstabodee, S.; Luengnaruemitchai, A. *J. Power Sources* **2006**, *163*, 547–554.
(19) Monyanon, S.; Pongstabodee, S.; Luengnaruemitchai, A. *J. Chin. Inst. Chem. Eng.* **2007**, *38*, 435–441.
(20) Tabakova, T.; Boccuzzi, F.; Manzoli, M.; Chiorino, A.; Andreeva, D.; Aldo Gamba, C. C.; Salvatore, C. *Studies in Surface Science Catalysis*; Elsevier: New York, 2005; Vol. 155, pp 493−500.

 10.1021/ja1028809

interest to develop a process able to yield an ultra pure hydrogen source for fuel cell applications. In this frame, intense investigations have been conducted during recent years, and especially gold-containing materials were reported as very promising catalysts to selectively convert CO into CO_2 in the presence of an excess of H_2.[1,18,19,21,22,24−29] In fact, gold has been for a long time disregarded for any catalytic applications because this noble metal is one of the most chemically inert element. The very new life of gold in heterogeneous catalysis is due to Haruta's pioneer work[30] who evidenced both a preparation method to obtain Au supported nanoparticles (mean diameter <5 nm) and the requirement of these nanosized gold particles to generate highly active catalytic sites. More precisely, the new coprecipitation method, which allows one to prepare gold nanoparticles with an optimal size around 3 nm,[31] even opened the door to the low temperature catalytic oxidation, because it appeared that CO could be converted into CO_2 at temperature as low as 200 K. From this discovery, the research on catalytic properties for gold has increased exponentially. Nevertheless, only a relative limited fraction of the reported studies deals with mechanistic investigations, and the majority of them concern CO oxidation at low temperature. These are the major reasons why this study focuses on Au/CeO_2 and Au/TiO_2 nanosized catalysts, aiming at understanding how they really work at the molecular scale to provide information useful for extending their efficiency to the oxidation of molecules more complex than CO, that is, VOC compounds, represented by methanol in the present case.

2. Experimental Section

Materials. The catalysts were prepared by depositing Au (via trihydrated chlorauric acid) onto CeO_2 and TiO_2 commercial powder materials with granulometry in the micrometer range. Two ceria supports with pure fluorine phase having a high and a low level of initial specific surface area and a pure anatase titania support were chosen for this study. Details on the sample preparation are reported in the Supporting Information.

In both cases, Au is finely dispersed onto the oxide supports with a mean particle size below 3 nm as estimated by the X-ray diffraction line broadening of Au. Furthermore, the specific surface area of the oxides was unaffected by the Au deposition, as described in Table 1.

Operando Tests. Operando IR studies were carried out using the transmission technique to obtain quantitative data. Sample and gas-phase IR spectra were alternatively collected to follow both the sample modifications and the methanol conversion, which was also measured by online mass spectrometry.

Table 1. Some Physicochemical Properties of the Studied Samples

sample name	gold content/ wt %	specific area (BET)/$m^2\ g^{-1}$	gold particles size/nm
TiO_2		85	
CeO_{2HSA}		180	
Au/TiO_2	0.6	85	<3
Au/CeO_{2HSA}	1	180	<3
Au/CeO_{2LSA}	1	60	<3

Details on the operando system and the applied methodology are reported in the Supporting Information. For this specific study requiring efficient thermal regulation at temperatures close to room temperature, a new reactor cell has been designed in our laboratory (Figure 1). It is made of a stainless steel cylinder that carries a toroidal sample holder in its center, where the catalyst is placed in the form of a self-supported wafer of 10 mg cm^{-2}. The thermoregulating system allows one to hold the sample at a fixed temperature in a range from 263 to 373 K. The reaction chamber hosting the sample is obviously tight with respect to the external atmosphere, and its dead volume is extremely small allowing one to obtain (i) time-resolved analysis, (ii) surface spectra without superposition of the gas-phase signal, and (iii) fluid dynamics very similar to that of a honeycomb system.

The reacting gas mixture composition was fixed to 700 ppm CH_3OH, 20 vol % O_2 in argon, and the total flow was adjusted to work with a constant gas hourly space velocity (GHSV) equal to 60 000 h^{-1}. Before any experiment, each sample was simply treated with argon and oxygen for a night at room temperature to stabilize the surface state, without any thermal activation, to prevent metal particle growth.

3. Results and Discussion

3.1. Effect of the Support CeO_2 or TiO_2. The first aim of this study was to investigate a potential activity of the support oxides themselves. The evolution of the CH_3OH conversion (calculated from IR gas-phase analysis) with time on stream (TOS) is given for CeO_2-based samples in Figure 2. Focusing on the CeO_{2HSA} sample, a conversion loss to reach a plateau without any catalytic activity was observed. Two hypotheses are possible to explain this phenomenon of conversion drop: (i) the catalysts deactivate with time on stream or (ii) the disappearance of CH_3OH is related to adsorption only and stops when the surface is saturated.

The upper part of Figure 2 indicates that during the first 30 min, the exposed surface cerium cations are saturated by methoxy species coming from the dissociative methanol adsorption. According to abundant literature data,[32−37] the band evolving at 1102 cm^{-1} is associated with the formation of on top methoxy species (type I) on Ce^{4+} cations, thus giving evidence that after one night pretreatment under oxygen at room temperature the main part of surface cations is oxidized. During

(21) Avgouropoulos, G.; Ioannides, T.; Papadopoulou, C.; Batista, J.; Hocevar, S.; Matralis, H. K. *Catal. Today* **2002**, *75*, 157–167.
(22) Avgouropoulos, G.; Papavasiliou, J.; Tabakova, T.; Idakiev, V.; Ioannides, T. *Chem. Eng. J.* **2006**, *124*, 41–45.
(23) Tabakova, T.; Boccuzzi, F.; Manzoli, M.; Sobczak, J. W.; Idakiev, V.; Andreeva, D. *Appl. Catal., A* **2006**, *298*, 127–143.
(24) Avgouropoulos, G.; Manzoli, M.; Boccuzzi, F.; Tabakova, T.; Papavasiliou, J.; Ioannides, T.; Idakiev, V. *J. Catal.* **2008**, *256*, 237–247.
(25) Ko, E.-Y.; Park, E. D.; Seo, K. W.; Lee, H. C.; Lee, D.; Kim, S. *Catal. Today* **2006**, *116*, 377–383.
(26) Luengnaruemitchai, A.; Osuwan, S.; Gulari, E. *Int. J. Hydrogen Energy* **2004**, *29*, 429–435.
(27) Panzera, G.; Modafferi, V.; Candamano, S.; Donato, A.; Frusteri, F.; Antonucci, P. L. *J. Power Sources* **2004**, *135*, 177–183.
(28) Manzoli, M.; Avgouropoulos, G.; Tabakova, T.; Papavasiliou, J.; Ioannides, T.; Boccuzzi, F. *Catal. Today* **2008**, *138*, 239–243.
(29) Wang, H.; Zhu, H.; Qin, Z.; Wang, G.; Liang, F.; Wang, J. *Catal. Commun.* **2008**, *9*, 1487–1492.
(30) Haruta, M.; Kobayashi, T.; Sano, H.; Yamada, N. *Chem. Lett.* **1987**, *16*, 405.
(31) Haruta, M. *CATTECH* **2002**, *6*, 102.
(32) Colón, G.; Pijolat, M.; Valdivieso, F.; Vidal, H.; Kašpar, J.; Finocchio, E.; Daturi, M.; Binet, C.; Lavalley, J. C. *J. Chem. Soc., Faraday Trans.* **1998**, *94*, 3717.
(33) Finocchio, E.; Daturi, M.; Binet, C.; Lavalley, J. C.; Blanchard, G. *Catal. Today* **1999**, *52*, 53.
(34) Daturi, M.; Binet, C.; Lavalley, J. C.; Galtayries, A.; Sporken, R. *Phys. Chem. Chem. Phys.* **1999**, 5717.
(35) Daturi, M.; Finocchio, E.; Binet, C.; Lavalley, J. C.; Fally, F.; Perrichon, V.; Vidal, H.; Hickey, N.; Kašpar, J. *J. Phys. Chem. B* **2000**, *104*, 9186.
(36) Binet, C.; Daturi, M. *Catal. Today* **2001**, *70*, 155. 155.
(37) Binet, C.; Daturi, M.; Lavalley, J. C. *Catal. Today* **1999**, *50*, 207.

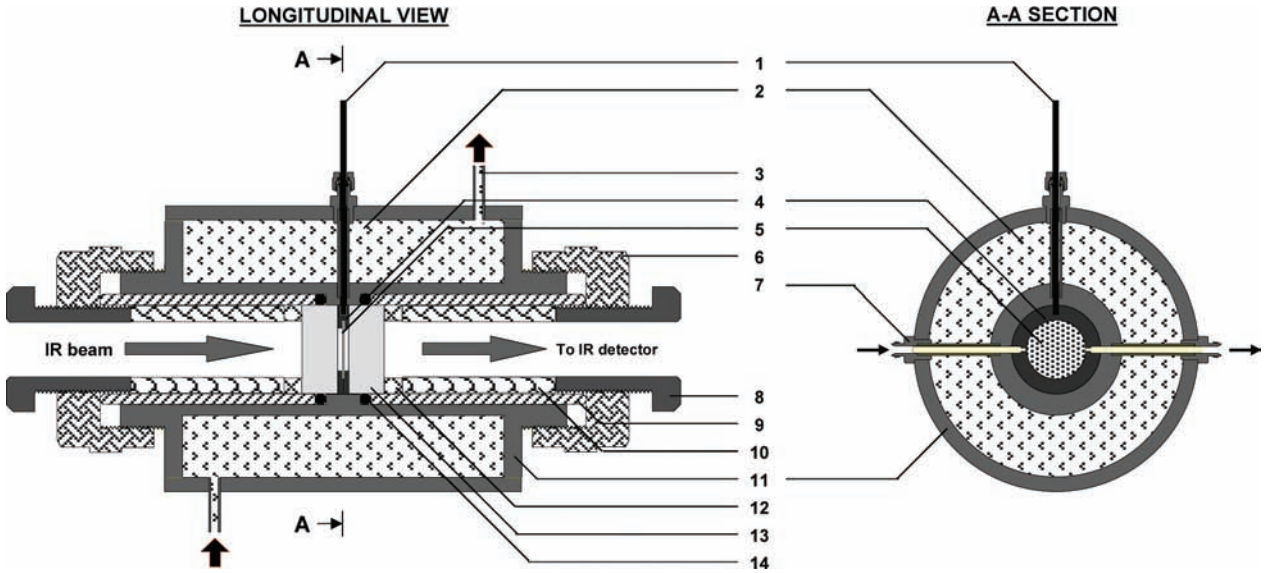

Figure 1. Detailed view of the CIRCOPE IR operando cell: (1) thermocouple, (2) oil tank, (3) oil circulation port connected to the cryostat, (4) wafer holder (stainless steel), (5) sample (wafer), (6) adjusting nut for air-tightness, (7) gas flow port, (8) adjusting nut for KBr windows, (9) stainless steel ring, (10) Teflon ring, (11) stainless steel cell body, (12) PEEK ring, (13) KBr window, and (14) Kalrez O-ring.

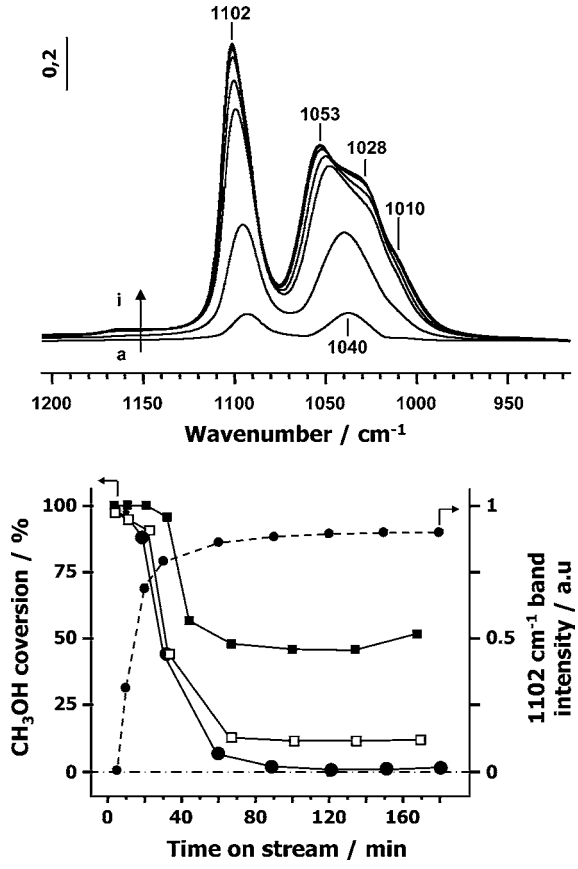

Figure 2. Bottom: Evolution of the methanol conversion (—) and the 1102 cm^{-1} band intensity (- - - -) with time on stream when the reaction is conduced over CeO_{2HSA} at (●) 323 K or Au/CeO_{2HSA} at (□) 298 K and (■) 323 K. GHSV = 60 000 h^{-1}, 700 ppm CH_3OH/20% O_2 in Ar. Top: FTIR subtraction spectra (the spectrum of the surface before reaction was subtracted for clarity seek) of adsorbed species on CeO_{2HSA} upon increasing time on stream at 323 K: (a) 5 min, (b) 10 min, (c) 20 min, (d) 30 min, (e) 60 min, (f) 90 min, (g) 120 min, (h) 150 min, and (i) 180 min.

the first 10 min under stream, another band centered at around 1040 cm^{-1} grows conjointly with the 1102 cm^{-1} one. That is assigned to the methoxys doubly bridging Ce^{4+} cations having an oxygen vacancy in the neighborhood (type II′ according to Badri et al.[38]). For higher times on stream (>10 min), the amount of adsorbed methanol keeps on increasing, and new bands in the doubly bridging methoxy region (1053 and 1028 cm^{-1}) emerge due to the coverage level effect. The first band is due again to type II methoxys, that is, bridged species on Ce^{4+} cations, whereas the second band would characterize nondissociative methanol physisorption.[39] A shoulder at 1010 cm^{-1} typical for traces of triply bridging methoxy species (type III)[37] is detected for the highest coverage level. Both the position of the doubly bridging methoxy bands (1053 instead of 1065 cm^{-1}, as expected for an oxidized ceria) and the relative intensity of the type III methoxy species slightly differ from spectra previously reported for methanol adsorption on pure CeO_2.[38] These discrepancies may be due to the presence of remaining adsorbed water and carbonate species (which may perturb other adducts), because no thermal pretreatment was performed. Finally, considering the band intensities, it is noticeable that when the methanol adsorption equilibrium is reached, the peak of type I methoxy band at 1102 cm^{-1} is around 1.5 times higher than that relative to type II. Comparing the evolution of the methoxy bands (lower part of Figure 2) with the profile of the mass spectra reported in Figure 3A, it is evident that once the surface is fully covered (30−40 min), the methanol level in the exhaust gas is the same as that at the inlet, while there is no CO_2 production, thus indicating that there is no catalytic conversion. Therefore, we can conclude that on the ceria support the disappearance of CH_3OH is related to adsorption only. However, the $m/z = 18$ signal (typical for H_2O) is increasing during the very first time on stream to go through a maximum and further decrease to the zero level when the surface equilibrium is reached. This phenomenon arises from the surface dehydroxylation upon replacement of OH groups by methoxys.

A quantitative confirmation for pure adsorption phenomena occurring with CeO_{2HSA} was obtained from an estimation of

(38) Badri, A.; Binet, C.; Lavalley, J. C. *J. Chem. Soc., Faraday Trans.* **1997**, *93*, 1159.
(39) Meyer, R.; Gunthard, H. S. *J. Mol. Spectrosc.* **1974**, *52*, 94.

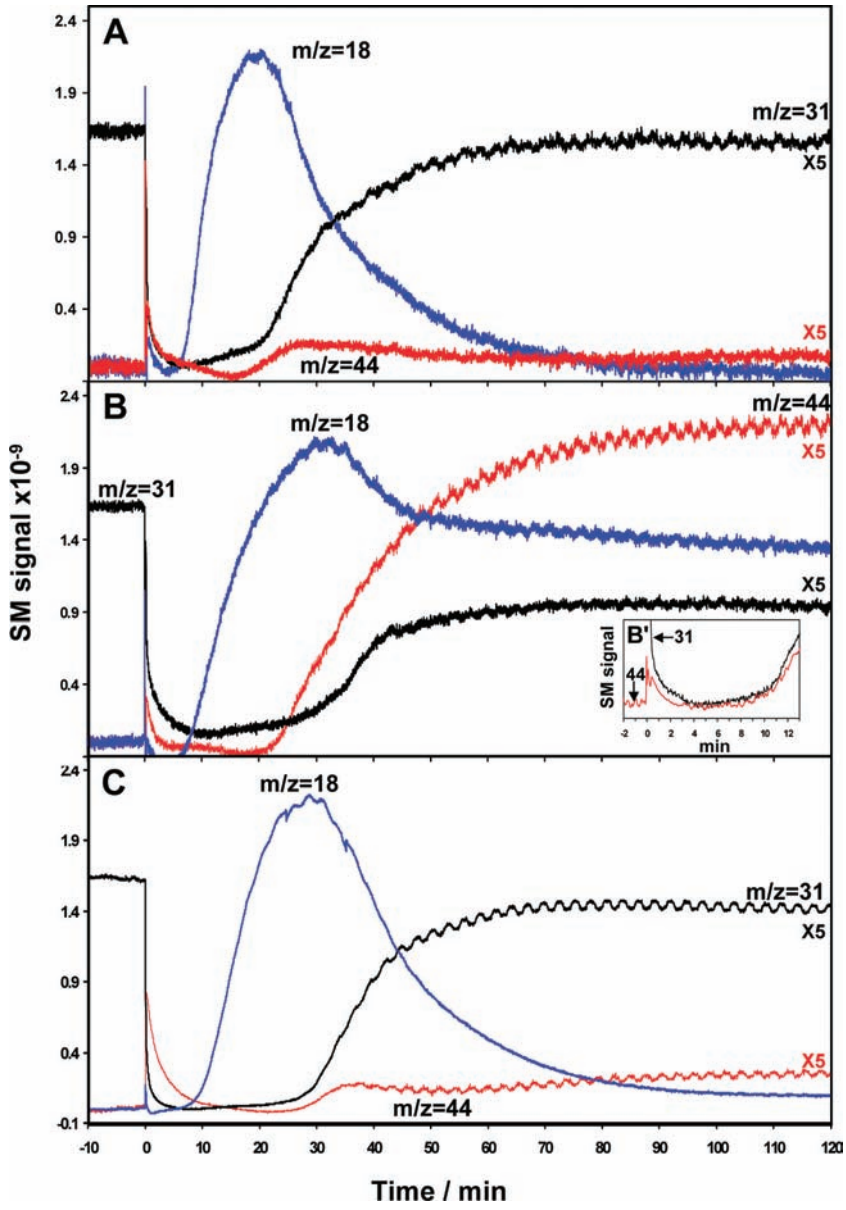

Figure 3. Evolution of mass spectra signal ($m/z = 31$ for methanol, 18 for water, 44 for CO_2) intensities with time on stream [GHSV = 60 000 h^{-1}; flow: 700 ppm CH_3OH + 20% O_2 (when present) in Ar, $T = 323$ K] when the reaction is performed over (A) CeO_2, (B) Au/CeO_{2HSA}, (B′) Au/CeO_{2LSA}, and (C) Au/CeO_{2HSA} without O_2.

the amount of adsorbed methanol under reaction flow. Indeed, it was found that when the equilibrium is reached (plateau regime), the coverage level almost corresponds to a monolayer in which methoxy species are in close contact with their neighbors. The details for the calculation are provided in the Supporting Information.

The same trend for both the gas-phase data and the surface species evolution was observed for TiO_2 and Au/TiO_2 catalysts, confirming that for CeO_{2HSA}, TiO_2, and Au/TiO_2 samples, the initial apparent conversion is only due to adsorption phenomena. For brevity's sake, all of the catalytic data concerning TiO_2-based samples are not reported here but are available in the Supporting Information.

3.2. Effect of Gold Nanoparticles on CeO_2. Contrarily to the pristine support, when gold nanoparticles are deposited on ceria, the activity stabilizes to a nonzero conversion (Figure 2). This result indicates an efficient catalytic activity for Au/CeO_{2HSA} sample in methanol oxidation, which is confirmed by a higher conversion (evaluated after 1 h of TOS when the activity is stabilized) at 323 K (50% calculated from IR online gas-phase analysis) than at 298 K (15%). The synergetic effect between the CeO_2 support and the gold nanoparticles will be discussed next.

In more detail, Figure 3B represents the MS data obtained for CH_3OH oxidation at 323 K over Au/CeO_{2HSA}: coherently with the IR analysis, the high initial CH_3OH consumption progressively decreases to reach a steady state after around 40 min on stream. The $m/z = 18$ water signal is detected starting from around 5−10 min, as it was the case for the Au-free CeO_2 (Figure 3A), and during the first 20 min on stream, both CeO_{2HSA} and Au/CeO_{2HSA} present the same MS signal evolution. In particular, the $m/z = 44$ associated with CO_2 remains close to zero, indicating in both cases that only methanol dissociative adsorption first takes place leading to water release. On the contrary, starting from 20 min on stream, an obvious gold effect appears, because CO_2 starts to be produced while the methanol

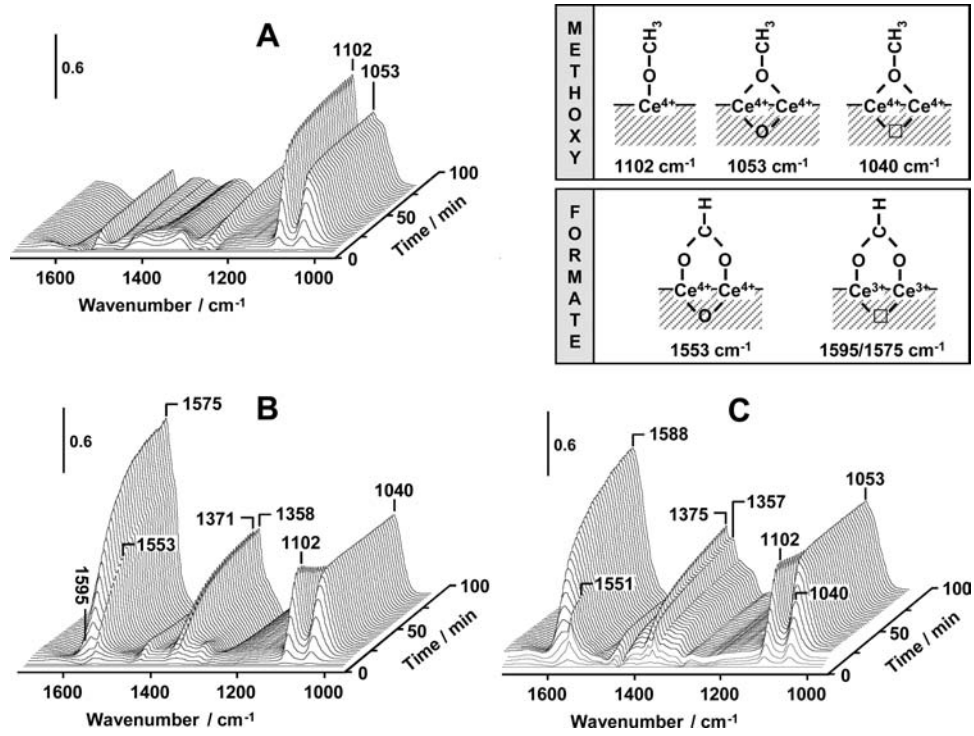

Figure 4. FTIR subtraction spectra in the δ(CH) and ν(CO) vibration range (the spectrum of the surface before reaction was subtracted for clarity seek) of adsorbed species with time on stream [GHSV = 60 000 h^{-1}; flow: 700 ppm CH_3OH + 20% O_2 (when present) in Ar, T = 323 K] when the reaction is performed over (A) CeO_2, (B) Au/CeO_{2HSA}, and (C) Au/CeO_{2HSA} without O_2.

signal tends toward a stabilized value around 50% of the bypassed level. This clearly indicates that the CO_2 formation is delayed when compared to the H_2O formation and would suggest that the methanol conversion proceeds in consecutive steps. Operando technique was then applied to observe the catalyst surface while working; the evolution of the adsorbed species with time on stream should provide further information about these consecutive steps.

3.3. CeO_2 and Au/CeO_2: Evolution of Adsorbed Species with Time On Stream. The evolution with time on stream at 323 K of the spectra typical of adsorbed species over CeO_{2HSA} is reported in Figure 4A.

Concerning the methoxy species, their ν(CO) modes were already fully described in Figure 2: briefly, the type II are associated with the broad massif centered around 1053 cm^{-1}, while the type I are responsible for the highest intensity band at 1102 cm^{-1}. The bands around 1450 cm^{-1} are associated with the bending δ(CH) modes, while the "waves" effects observed between 1600 and 1200 cm^{-1} are due to perturbations with the already present adsorbed impurities (carbonates, water, etc., as detected on the surface spectra before sending the reactant flow).

In a similar way, the evolution of the spectra with time on stream at 323 K is reported for Au/CeO_{2HSA} in Figure 4B: new intense bands are observed at 1595, 1575, and 1553 cm^{-1}. These three bands correspond to the ν_a(OCO) vibrations of various adsorbed formate species. The 1595 and the 1575 cm^{-1} components are characteristic of $HCOO^-$ species on Ce^{3+} cations, whereas the lower wavenumber component at 1553 cm^{-1} is due to bidentate formate species on oxidized Ce^{4+}.[33,40] The 1595 and 1575 cm^{-1} bands being the most intense, the formate species' appearance is thus accompanied by Ce^{4+} reduction into Ce^{3+}. The cerium cations' reduction appears to be a very local consequence of the formate formation because no evidence of methoxy species coordinated with Ce^{3+} could be detected. The corresponding symmetric mode ν_s(OCO) is much less sensitive to the cerium cation oxidation degree so that only one band is detected at 1358 cm^{-1} for the formates. To complete the formate species characterization, the 1371 cm^{-1} band can be assigned to their δ(CH) mode.[33] It is worth underlining that all of the band assignments reported above are fully consistent with the vibration modes detected in the ν(CH) stretching region, which are exhaustively described in the Supporting Information.

Considering now the ν(CO) vibration modes for methoxy species, the wavenumbers observed during reaction are rather the same as those observed upon the first instants of adsorption on the bare CeO_2 support (when there is no shift due to coverage effect), that is, at 1102 and 1042 cm^{-1} for type I and type II′ methoxys, respectively. Moreover, when the reaction takes place over Au/CeO_{2HSA}, the peak height for the type I methoxy band is always lower than that relative to the type II′ methoxy, whereas it was almost double in the case of pure adsorption on the bare CeO_2 (Figures 2 and 4A). One may wonder if this is due to the fact that Ce^{4+} sites are less accessible in the presence of supported Au. Knowing the gold weight loading, the deposited gold particles mean size (S_m < 3 nm; see Table 1), and the support specific area, it is deduced that less than 0.5% of the CeO_2 surface is thus occupied by Au nanoparticles (calculation details are provided in the Supporting Information). Thus, the much lower amount of type I methoxy observed during reaction over Au/CeO_{2HSA} cannot be explained by a much lower number of Ce^{4+} adsorption sites due to Au nanoparticles deposition. This last result indicates that, under reaction flow, the surface never reaches methoxy saturation and suggests that

(40) Binet, C.; Jadi, A.; Lavalley, J. C. *J. Chim. Phys. Phys.-Chim. Biol.* **1992**, *89*, 1441.

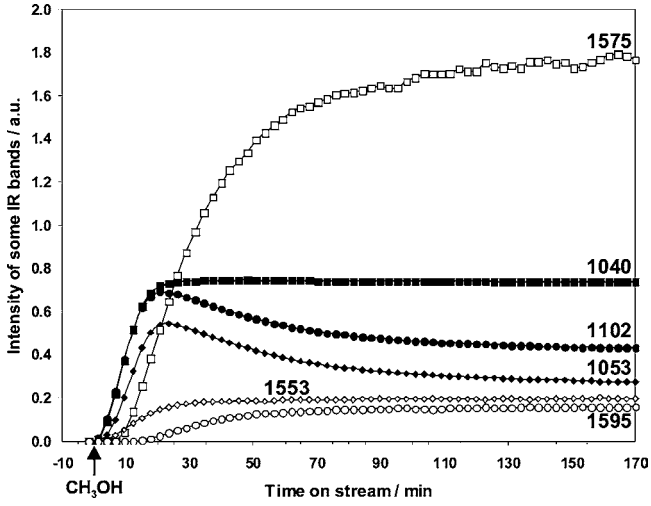

Figure 5. Evolution of selected IR bands typical of adsorbed species on Au/CeO_{2HSA} catalyst with time on stream at 323 K (700 ppm CH_3OH + 20% O_2 in Ar). The curve labeling refers to the corresponding band wavenumber in cm^{-1}.

type I methoxy are continuously transformed, playing probably a key role in the catalytic methanol oxidation.

To further investigate this possible methoxy key role, the evolution of the intensity of characteristic bands upon TOS has been reported for the Au/CeO_{2HSA} (Figure 5). The 1040 cm^{-1} ν(CO) band, typical of type II′ methoxy, presents the same feature for Au/CeO_2 and for CeO_2, characterized by a plateau (see Figures 4 and 5).

On the contrary, the 1102 cm^{-1} component typical of type I methoxy now goes through a maximum for the Au/CeO_2 catalyst. This trend is typical for an intermediate species whose transformation starts when a critical concentration (here surface coverage) is reached. The decrease of the amount of type I methoxy on the surface corresponds to the significant appearance of the new bands typical for formate species at 1553, 1575, and 1595 cm^{-1}, which were not observed on the bare supports nor on Au/TiO_2 (not reported here). The fact that during reaction over Au/CeO_{2HSA} the type I methoxy band intensity never reaches the same level as that observed upon adsorption equilibrium over the bare CeO_{2HSA} is thus due to the oxidation of type I methoxy into formate species. Moreover, the 1053 cm^{-1} mode typical of type II methoxys is hardly observed over Au/CeO_2 under both CH_3OH and O_2 flow (Figure 4B), which also suggests their transformation into formates in these conditions. Indeed, the 1053 and 1040 cm^{-1} bands are overlapping, and the intensity of the former is low so that its evolution is better described in Figure 5. Actually, it then appears that both type I and type II methoxy species have parallel evolution under methanol and oxygen flow, thus indicating similar reactivity in these conditions. On the contrary, the type II′ methoxy band intensity at 1040 cm^{-1} seems to remain stable when formate species are formed (compare Figure 4A and B and refer to Figure 5). This can be justified by the fact that the environment of type II′ species is oxygen deficient, being therefore unable to oxidize methoxy to formate species, whereas type I and type II are coordinated to cations bearing a complete oxygen 8-fold coordination. This oxygen needs the presence of a metal (i.e., Au in our case) to be activated at low temperature, leading to an increased surface and subsurface mobility via a reverse spillover effect as reported by Leppelt et al., who also concluded that a catalytic active perimeter (the so-called "adlineation sites") should be present at the interface between gold and the support.[41] Working on the hypothesis of a catalytic reaction through a Mars van Krevelen mechanism, the oxygen atoms consumed for methanol oxidation are replaced in the oxide support surface vacancies by oxygen molecules from the gas phase. More precisely, we propose that, at room temperature and at the adlineation sites, the Au role consists of enabling the Ce^{3+} formate formation from ceria surface oxygen species, which further generates surface vacancies acting as oxygen pumps (reverse spillover effect). It would also be tempting to propose that the atomic active oxygen species necessary to transform methoxys into formates are provided by a direct oxygen molecule dissociation onto gold nanoparticles. This possibility was in fact proposed by Schubert et al. in their elegant study on the role of inert and active support materials for the oxygen supply: according to them for Au supported on inert materials, the oxygen supply would most likely proceed via direct dissociative adsorption on the Au particles, while for Au catalysts supported on active materials (such as CeO_2) the dominant reaction pathway would involve the adsorption of a mobile, molecular oxygen species on the support with a further dissociation at the interface with gold nanoparticles.[42] The last conclusion should be relevant to this work for which the ceria support is known to possess an active redox surface acting as an oxygen buffer. Moreover, the hypothesis of O_2 direct dissociation onto gold was here disregarded, because, to our knowledge, no proof of such a dissociative adsorption has been clearly provided.

Effect of Anaerobic Conditions. To illustrate the role of the ceria mobile oxygen species, a similar experiment was conducted with an anaerobic flow. In these conditions, the methanol dissociative adsorption also takes place, as indicated by the water yield (Figure 3C, $m/z = 18$), but then the conversion evolution is similar to that observed for pure CeO_2 experiment (Figure 3A), that is, without any further oxidation product detected in the gas phase ($m/z = 44$). Focusing on the surface (Figure 4C), some formates are however detected. Scrutinizing in depth the spectra, a similar decline (although softer) of type I methoxy was detected. This decrease corresponds to the formate appearance (associated with the ceria buffered oxygen species consumption), but both type II and type II′ reach a plateau without any further decrease; their oxidation into formates involving a neighboring surface or subsurface oxygen is prevented due to a limited oxygen availability/mobility related to the absence of O atoms (from the gas phase) able to re-equilibrate the solid anionic content.

This methanol oxidation mechanism going through formate species was already observed on CeO_2-based samples, but at higher temperatures of 423−473 K.[33] As aforementioned, the gold nanoparticles would presumably increase the ceria oxygen mobility, likely via a reverse spillover effect, thus decreasing the methanol oxidation energy barrier and making it possible at a lower temperature than on the bare support.

3.4. Methanol to CO_2 Mechanism over Au/CeO_2. The aim for any operando experiment is to make the link between gas phase and surface analysis data. For this purpose, selected time on stream ranges will be considered, dealing first with the experiment over Au/CeO_2 at 323 K in the presence of both CH_3OH and O_2.

(41) Leppelt, R.; Schumacher, B.; Plzak, V.; Kinne, M.; Behm, R. J. *J. Catal.* **2006**, *244*, 137–152.
(42) Schubert, M. M.; Hackenberg, S.; van Veen, A. C.; Muhler, M.; Plzak, V.; Behm, R. J. *J. Catal.* **2001**, *197*, 113–122.

(i) From zero to around 10 min on stream, the methanol conversion is stable around 100%, but no reaction products are observed in the exhaust gas stream (see Figures 2 and 3B). Analysis of the surface data evidenced accumulation of methoxys on the catalyst (types I, II, and II′ as described on Figures 4B and 5), indicating that methanol removal from the gas phase is mostly due to dissociative adsorption. Indeed, only traces of formates are detected on the surface during this period.

(ii) From 10 min to around 45 min TOS, the conversion drops from 100% to stabilize around 50%. This phenomenon is accompanied by water and CO_2 production (Figure 3B), indicating that catalytic reactions start to proceed during this step. However, a delay between water and CO_2 production is observed attributed to first H_2O release upon methanol dissociative adsorption and then to methoxy oxidation. The real catalytic reaction, evidenced by CO_2 release, takes place after 20 min TOS, as confirmed by surface data showing methoxy species decrease concomitant with formate accumulation on the catalyst, which become the principal species in the infrared spectra (Figures 4B and 5). At this step of the study, one can wonder from Figures 3 and 4 why the monolayer (made of both methoxys and formates) should be practically established to observe a consistent catalytic activity (CO_2 production). Considering the calculation reported in the Supporting Information, the gold nanoparticles only account for 0.5% of the catalyst area. Because it has been shown that the presence of gold nanoparticles is necessary for catalytic activity, the active sites must thus be on the metal itself or in its close neighborhoods. Therefore, the reactants must first reach those sites before undergoing any further reaction than single dissociative adsorption. Being at relatively low temperature, the species diffusivity at the surface is limited, and statistically only a fully covered surface allows one to obtain the required proximity to initiate the reaction. Aiming at checking this point, the Au/CeO_2 LSA sample having the same gold loading but a support surface area lowered to one-third was tested. As expected, the sample oxidation activity evidenced by CO_2 formation started at a time roughly 3 times shorter (compare Figure 3B with B′); the surface full coverage (characterized here by a total amount equal to one-third of those on Au/CeO_{2HSA}) is therefore a prerequisite for initiating the oxidation reaction. This fact is again in perfect agreement with the existence of an "active perimeter" at the interface between Au nanoparticles and the oxide support,[41] which must be reached to allow species catalytic conversion.

As a summary for phenomenon occurring until 45 min TOS, eq 2 indicates that the transformation of type I methoxy is accompanied by both H_2O production and Ce^{4+} reduction into Ce^{3+} (with a concomitant H_2 production, as previously evidenced[33]), the whole being consistent with our data.

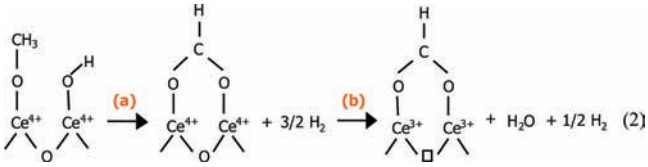

(2)

For type II methoxy species, the mechanism is practically the same, but will not be detailed here for the sake of brevity. Note that in our case where the working atmosphere is oxygen containing, H_2 is consumed in the catalytic cycle and is not detected in the gas exhaust stream.

(iii) Finally, for time on stream above 45 min, the conversion remains stable around 50% (Figure 3); the complete catalytic methanol oxidation reaches the steady state. The surface data indicate that starting from around 45 min, the surface equilibrium between methoxy and formate species is almost achieved, and the formate accumulation rate slows as indicated in Figure 5 by the slope change. At this step, we can hardly distinguish whether formates are bare spectator species or reaction intermediates. Some points are however in favor of the second hypothesis; because the formate species are accumulating on the surface and because the lowering of their accumulating rate corresponds to the presence of CO_2 as a reaction product, one can propose that the complete methanol oxidation-determining step consists of the formate transformation. In the case of the low temperature water gas shift reaction over similar catalysts, it was indeed reported that formates adsorbed on the ceria support act as reaction intermediates in the dominant reaction pathway[41] yielding CO_2 and H_2 (in oxygen-free atmosphere). Moreover, in the past, we already demonstrated on ceria-based compounds that methanol can be adsorbed and then oxidized through formate intermediates.[33] The different possibilities for formate transformation into CO_2 and H_2O were thus investigated.

The first possibility is the decomposition of formates into hydroxyls and CO as described by eq 3. As already described, step c would only occur when O_2 is present in the flow. Moreover, step d is consistent with the best known property of gold nanoparticles, which is to be very active for CO oxidation, as recently reviewed by C. Louis.[43] The second possibility is

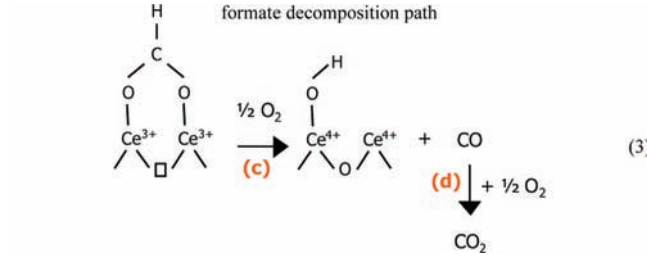

(3)

the direct formate oxidation (over Ce^{4+} or Ce^{3+}) requiring in one single step both surface dehydroxylation and neighboring cerium cation reduction, thus implying a global order of reaction higher than one according to eq 4.

$$HCOO^- + OH^- + 2Ce^{4+} \xrightarrow{(e)} CO_2 + H_2O + 2Ce^{3+} \qquad (4)$$

One way to determine which of the two proposed formate transformations is valid consists of tracking of the CO molecule, which is only involved in the decomposition mechanism (eq 3). As expected according to the very high CO oxidation reaction kinetics, the analysis of the gas-phase data never allowed one to give any evidence of carbon monoxide at the reactor outlet; however, focusing on the catalyst surface during reaction, the presence of CO adsorbed on gold nanoparticles was detected.

Figure 6 illustrates that the main bands that are observed in the 2300−2000 cm^{-1} region on both CeO_{2HSA} and Au/CeO_{2HSA} are located around 2280, 2200, and 2050 cm^{-1} (with slight shifts depending on the sample) and should be assigned to methoxy ν(CO) overtones and combination modes. This assignment is consistent with higher band intensities for the CeO_{2HSA} sample, which was shown to reach surface methoxy saturation, whereas the Au/CeO_{2HSA} sample transforms methoxys into formates.

(43) Louis, C. In *Nanoparticles and Catalysis*; Astruc, D., Ed.; Wiley-VCH: Weinheim, 2008; pp 475−503.

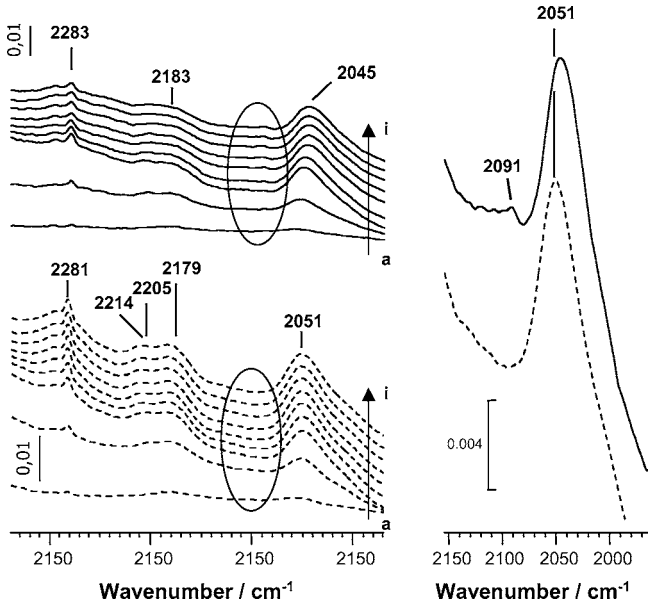

Figure 6. FTIR subtraction spectra (the spectrum of the surface before reaction was subtracted for clarity seek) of adsorbed species on (—) Au/CeO_{2HSA} catalyst and on (- - -) CeO_{2HSA} upon increasing time on stream: (a) 5 min, (b) 10 min, (c) 20 min, (d) 30 min, (e) 60 min, (f) 90 min, (g) 120 min, (h) 150 min, and (i) 180 min. The right part is an enlargement for both samples after 120 min. GHSV = 60 000 h^{-1}, 700 ppm CH_3OH + 20% O_2 in Ar, T = 323 K.

Considering the enlargement on the right part of Figure 6, the presence of a minor band at 2091 cm^{-1} is detected, which is only present for the gold-containing sample. According to the literature data,[44] this band should be assigned to CO adsorbed on gold nanoparticles possessing a metallic character. The very low intensity of this 2091 cm^{-1} band is consistent with a very low surface concentration of highly active intermediate CO-adsorbed species. Because adsorbed CO species were observed, the formate decomposition mechanism is proven to occur in our reaction conditions, and even if it is impossible to reject the direct oxidation pathway, we propose that the latter is minor. Furthermore, the direct oxidation pathway (eq 4) should give rise to CO_2 production even in the absence of oxygen, which was not the case, as observed in Figure 3C.

At this step of the study, enough information were obtained to propose a full description of the whole catalytic loop for the Au/CeO_2 catalyst. As depicted in Figure 7, the surface of the catalyst is initially covered by water and carbonate impurities; upon methanol dissociative chemisorption, water is desorbed and methoxys cover the surface. Three types of species are mainly observed: I, II, and II′. These species do not react anymore on the bare support at room temperature, whereas they undergo different transformations in the presence of gold nanoparticles.

(i) Type II′ methoxy species do not participate in any oxidation step, but they simply accumulate on the surface. On this basis, they can be considered as spectator species (bottom of Figure 7).

(ii) Type II species only react in the presence of oxygen: they give rise to formates, first on Ce^{4+} and then on Ce^{3+} cations, which constitute the redox pair necessary for the methoxy to formate oxidation. Successively formates decompose to desorb CO and leave an OH group on the surface, which comes back to its initial state. CO is further oxidized to CO_2 on gold nanoparticles, while the Ce^{3+} cations are reoxidized to Ce^{4+}, thus closing the catalytic loop (Figure 7, middle).

(iii) Type I species undergo the same transformation in the presence of oxygen (Figure 7, top right). They also react in anaerobic conditions; however, their oxidation stops after formates formation on Ce^{3+} (Figure 7, top left) when all of the available mobile oxygen atoms provided by the support have been consumed.

For the sake of clarity, we should underline that the $^3/_2H_2$, $^1/_2H_2$, or $^1/_2O_2$ species mentioned in the mechanism might be only entities necessary to equilibrate the reaction steps. In reality, these entities are probably provided by surface OH groups or capping oxygen atoms, but it would be too complicated to fully detail the mechanism.

Finally, emphasis should be made on the fact that for both type I and type II methoxy oxidation into formates, the proposed mechanism involves the participation of active atomic oxygen species, which are likely to form at the interface between gold nanoparticles and the ceria support.[42] This remark opens the door to propose an explanation for the Au/TiO_2 lack of activity in methanol oxidation at room temperature without contradicting its high efficiency in CO oxidation. Indeed, literature data relative to complementary oxygen isotope exchange and ESR experiments indicate that an Au/TiO_2 sample that is highly efficient in CO oxidation does not lead to any O_2 dissociation to atomic oxygen, but that on the contrary O_2 adsorbs onto TiO_2 oxygen vacancies to form active superoxide O_2^- species.[45]

3.5. Kinetics Considerations. Preliminary kinetics considerations are provided in the Supporting Information so that only the main results are reported here. Figure 8 indicates that an increase of the reaction temperature from 298 to 323 K at constant space velocity leads to an increase (around 50%) of the amount of adsorbed formate species. This seems a possible confirmation that formates are active intermediate species whose transformation is the rate-determining step. In fact, the steady-state concentration of formates on the surface is the result of their formation (methoxy conversion into formate) and their consumption (formate oxidation into CO_2). Both kinetic constants increase with higher temperature (Arrhenius law); therefore, if the formate concentration is enhanced, their formation increases faster than their oxidation, thus confirming the $HCOO^-$ oxidation as the rate-determining step.

The effect of the reaction temperature (at constant space velocity) on the conversion over Au/CeO_{2HSA} was described from Figure 2: at the steady state, the conversion increases from 15% at 298 K to 50% at 323 K. The activity was thus multiplied by more than a factor 3, while the active intermediate formate concentration was only multiplied by a factor 1.5. This result was expected due to the variation of the kinetic constant with the temperature, and an estimation of the apparent activation energy E_a of methanol oxidation over Au/CeO_{2HSA} sample was calculated according to eq 5:

$$E_a = -\ln\left(\frac{a_s(T_1)}{a_s(T_2)}.\frac{[HCOO^-]_{T2}}{[HCOO^-]_{T1}}\right)R\frac{T_1T_2}{(T_2 - T_1)} \qquad (5)$$

where $a_s(T_i)$ stands for the specific activity at the temperature T_i, $[HCOO^-]_{Ti}$ stands for the formate surface concentration at

(44) Henao, J. D.; Caputo, T.; Yang, J. H.; Kung, M. C.; Kung, H. H. *J. Phys. Chem. B* **2006**, *110*, 8689–8700.

(45) Liu, H.; Kozlov, A. I.; Kozlova, A. P.; Shido, T.; Asakura, K.; Iwasawa, Y. *J. Catal.* **1999**, *185*, 252–264.

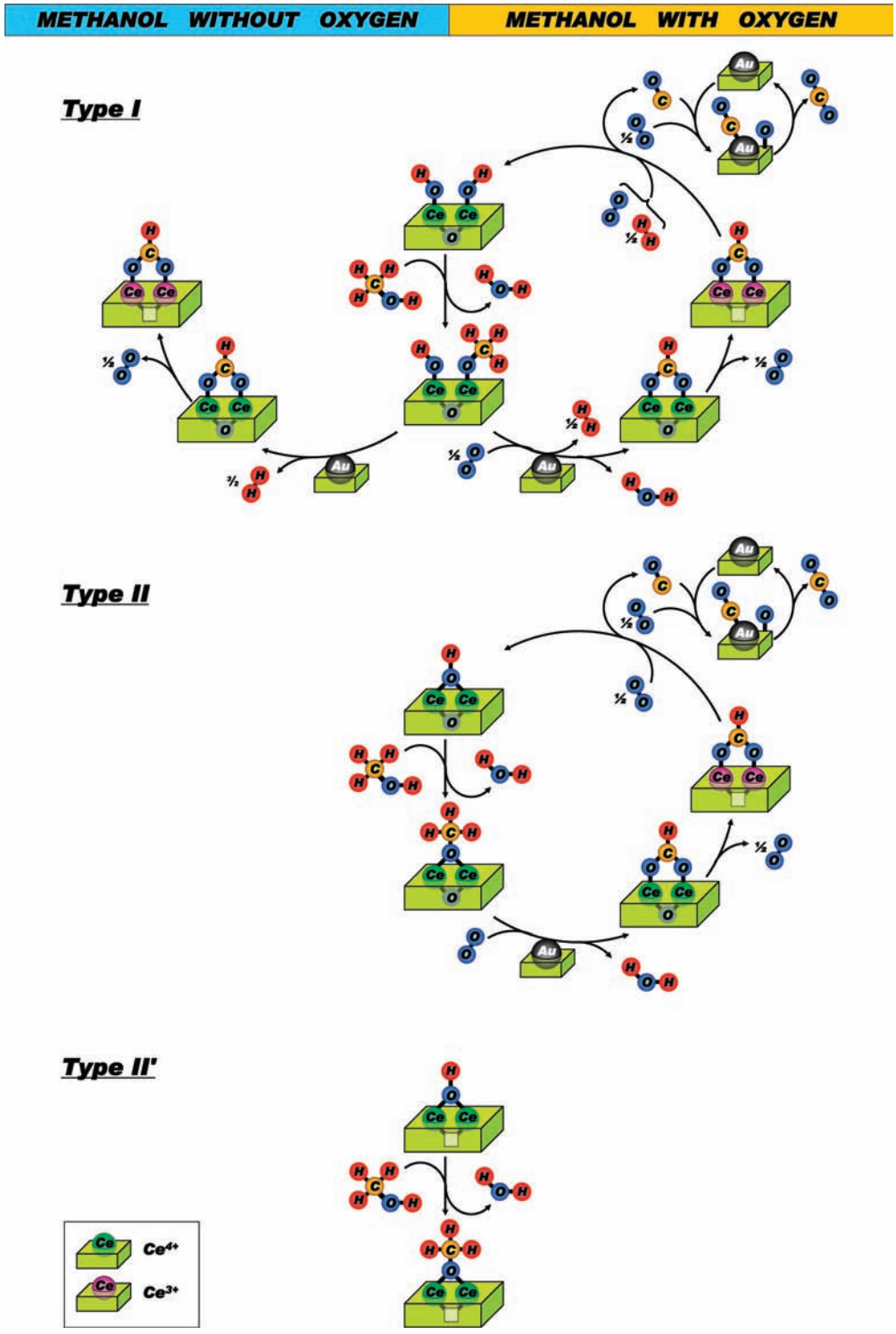

Figure 7. A sketch of the catalytic cycle for methanol oxidation over Au/CeO_2 sample. Reaction mechanism for the methoxy formation (type I, upper part; type II, middle part; type II′, bottom part), and then oxidation in the absence (left) or in the presence (right) of oxygen.

the temperature T_i, and $R = 8.314$ J K^{-1} mol^{-1}. The obtained apparent activation energy for the process is $E_a = 29$ kJ mol^{-1}, which is a relative small value when compared to some literature data. For example, iron formate oxidation with O_2 is reported to require an activation energy of 238 kJ mol^{-1}.[46] Elsewhere, Gates et al. reported that CO oxidation on gold-based catalysts presents an apparent activation energy of 138 or 54 kJ mol^{-1} depending on the metal particle size.[47] In both cases, the reported E_a values are much higher than the one obtained in the present study for a slower step. However, our E_a value (29 kJ mol^{-1}) is of the same order of magnitude (even slightly lower) that the one reported (40 kJ mol^{-1}) for the same rate-determining step over similar Au/CeO_2 catalysts.[41] These comparisons with

(46) Nobukawa, T.; Yoshida, M.; Kameoka, S.; Ito, S.; Tomishige, K.; Kunimori, K. *J. Phys. Chem. B* **2004**, *108*, 4071.

(47) Aguilar-Guerrero, V.; Gates, B. C. *J. Catal.* **2008**, *260*, 351–357.

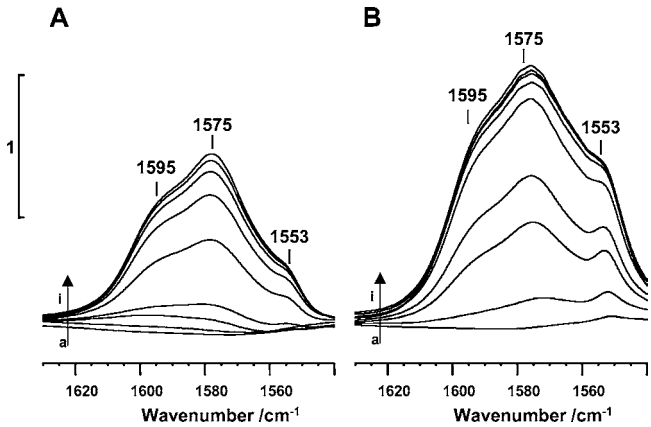

Figure 8. Effect of the reaction temperature (A) $T = 298$ K and (B) $T = 323$ K on the amount of adsorbed formate species on Au/CeO_{2HSA} during reaction. The IR spectra are given for the following time on stream: (a) 5 min, (b) 10 min, (c) 20 min, (d) 30 min, (e) 60 min, (f) 90 min, (g) 120 min, (h) 150 min, and (i) 180 min. GHSV = 60 000 h^{-1}, 700 ppm CH_3OH + 20% O_2 in Ar.

literature data thus clearly confirm that our Au/CeO_{2HSA} catalyst is very active for formate transformation and thus for methanol oxidation, when present as traces in ambient air even at room temperature.

4. Conclusions

In the present article, FTIR spectroscopy coupled with mass spectrometry was used to study the methanol oxidation mechanism at low temperatures on nanostructured Au/CeO_2 and Au/TiO_2 catalysts. The unique approach consisting of time-resolved simultaneous analysis of adsorbed and gaseous species allowed us to evaluate the activity and selectivity toward CO_2 and to identify consecutive steps in the oxidation pathway. Among all of the detected adsorbed species, type I and type II methoxys were evidenced as intermediates, which further transform into formates, whose oxidation was found to be the rate-determining step for the reaction. On the contrary, type II′ methoxys (possessing an oxygen vacancy in the neighborhoods) were proved to act as bare spectator species. Regarding the nature of the active sites, experiment on the pristine support proved without any doubt the necessity of gold to observe catalytic oxidation at room temperature. Furthermore, both the induction period required to observe real catalytic CO_2 production and the complementary experiments conducted in anaerobic conditions proved the relevance of the gold−support interface to initiate the low temperature catalytic reaction and the peculiarity of ceria as a redox support. In fact, no methanol oxidation was observed for gold over TiO_2 in such conditions, likely due to the absence of mobile atomic oxygen species on the latter compound surface.

We have also highlighted that the specific area of the ceria support is an important parameter to reach the steady-state conditions for the reaction: the methoxy surface coverage until around the monolayer appears necessary to initiate the CO_2 production, thus indicating that only a minor part of them are in the close neighborhoods of active gold−support interface sites. We must stress that it is really thanks to the spectroscopic survey of the catalysts under duty that we have been able to overcome the challenging experimental conditions, which would have impeached a traditional mechanism study from bare gaseous data. Moreover, not only the nature of adsorbates could be identified but also the study of their evolution versus time allowed one to distinguish whether they behaved as spectators or intermediates. However, intermediates' evolution may be different depending on their position in the pathway so that only the kinetic treatment of the spectroscopic data allowed one to point out formate decomposition as the rate-determining step.

Finally, a comparison with some literature data highlighted the outstanding performances of the investigated Au/CeO_2 materials as catalysts for VOC removal at ambient conditions and permits us to propose them as reliable devices for confined atmosphere purification.

Supporting Information Available: Experimental section including sample preparation procedure and conditions for catalytic operando tests. Results and discussion section containing TiO_2-based samples catalytic activity and estimation of the methoxy monolayer over CeO_{2HSA}; description of the ν(CH) vibration range relative to Figure 4 and estimation of the gold surface concentration; and hypotheses used for kinetic calculations. This material is available free of charge via the Internet at http://pubs.acs.org.

JA1028809